Supplementary Information

Significantly enhanced capacitive energy-storage performance of a flexible P(VDF-CTFE)-polyimide bilayer by optimizing the interface effect

Shaoyan Zhang[1], Bing Xie[1]*, Haishan Xu[1], Jinqiao Yi[2]*, Kun Guo[1], Haibo Zhang[3,4], Tianyu Li[5,6]*

[1]School of Power and Energy, Jiangxi Key Laboratory of Green General Aviation Power, Nanchang Hangkong University, Nanchang 330063, China

[2]College of Intelligent Systems Science and Engineering, Hubei Minzu University, Enshi 445000, China

[3]School of Materials Science and Engineering, Huazhong University of Science and Technology, Wuhan 430074, China

[4]Huangpu Institute of Materials, Guangzhou 510530, China

[5]School of Materials Science and Engineering & Beijing Advanced Innovation Center for Materials Genome Engineering, University of Science and Technology Beijing, Beijing 100083, China

[6]Department of Physics, City University of Hong Kong, Kowloon, Hong Kong, China

*Corresponding authors: xieb@nchu.edu.cn (Bing Xie); 2006009@hbmzu.edu.cn (Jinqiao Yi); tianyuli@ustb.edu.cn (Tianyu Li)

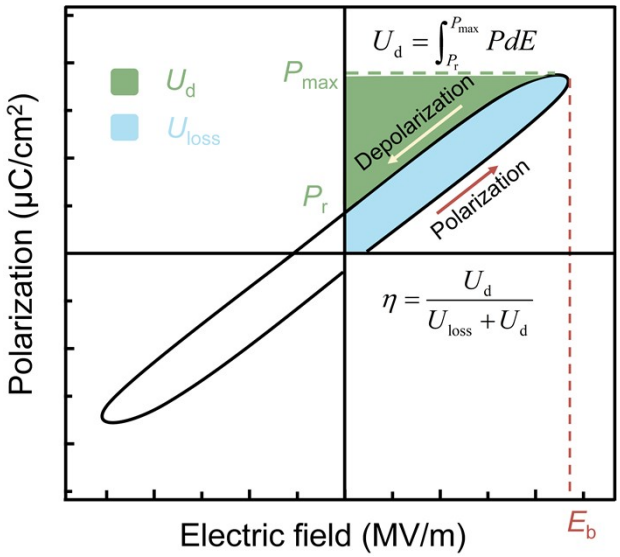

Fig. S1. Schematic *P*–*E* loops used for the calculation of discharge energy density and efficiency. It can be divided into two processes: polarization and depolarization. Among them, the area in green in the figure represents U_d, and the area in blue represents energy loss (U_{loss}).

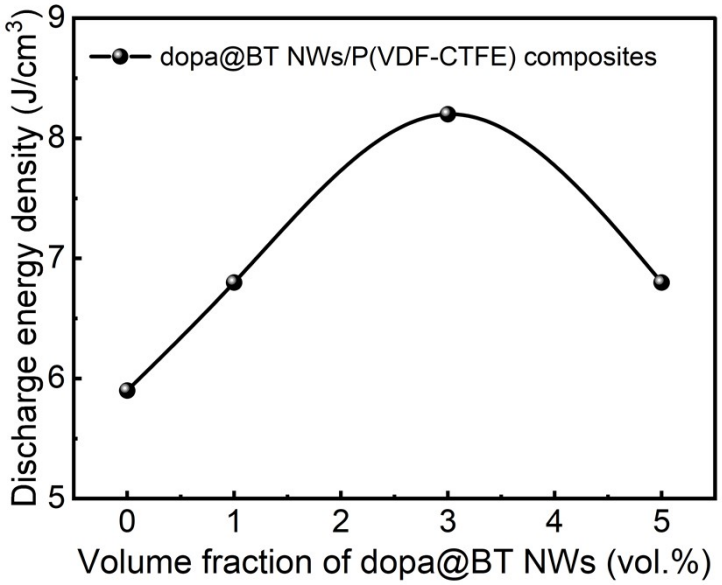

Fig. S2. Discharge energy densities of the P(VDF-CTFE)-based nanocomposites containing different volume fractions of dopa@BT NWs.

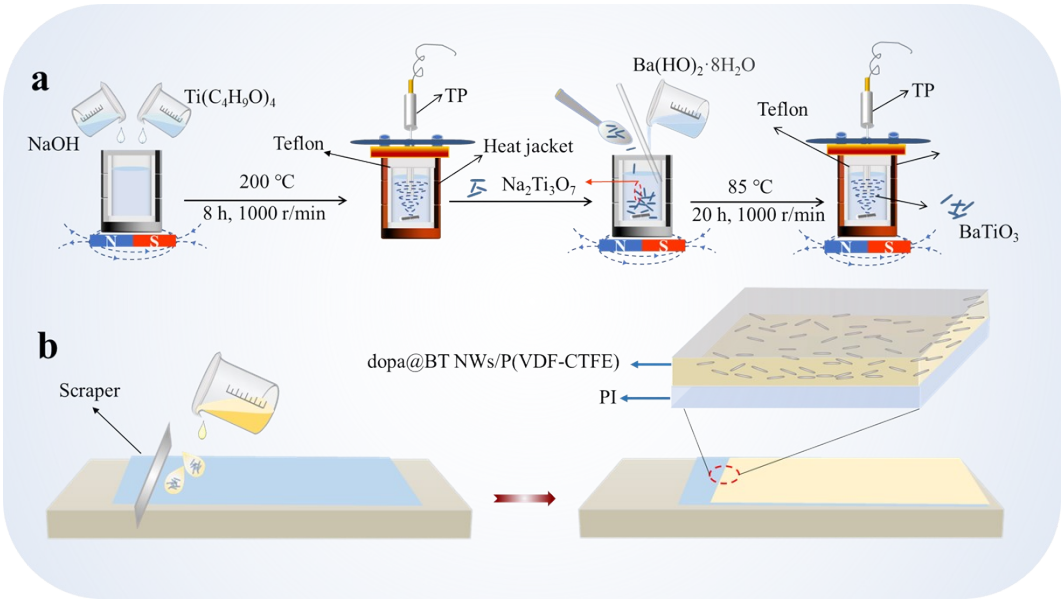

Fig. S3. Schematic diagram of (a) the preparation of $BaTiO_3$ nanowires and (b) nanocomposite bilayers.

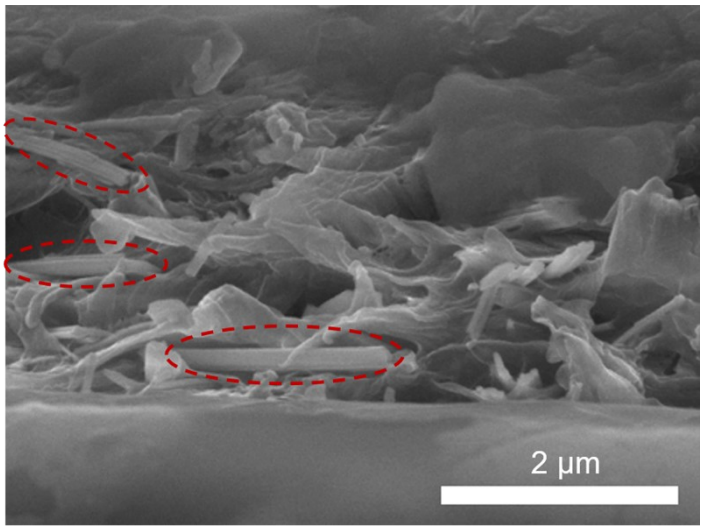

Fig. S4. Cross-sectional localized high-resolution magnified SEM image of the 8dBP-8PI nanocomposite. Due to the excellent low-temperature and high-temperature stability of the PI film, it can be used for a long time at temperatures ranging from −200 to 300 ℃, and it will not crack even in liquid helium at −269 ℃. Therefore, the conventional liquid nitrogen quenching method for preparing SEM cross-sectional samples is not applicable for preparing the 8dBP-8PI composite film cross-section. To overcome this, we adopted the rapid cutting method using ultra-thin blades to prepare the 8dBP-8PI nanocomposite film cross-section. The specific procedure was as follows: The 8dBP-8PI layered nanocomposite film was placed on a polytetrafluoroethylene plate, and then it was rapidly cut using an ultra-thin blade to obtain a cross-section suitable for microscopic morphology observation.

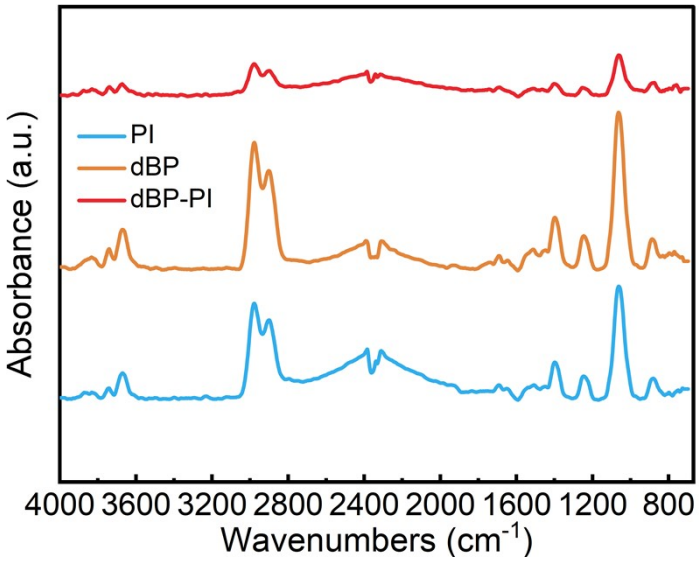

Fig. S5. FTIR spectra of PI, dBP, and dBP-PI films.

Table S1. Ferroelectric properties of *x*dBP-8PI nanocomposites and the local electric field strength in layers of different thicknesses.

Samples	E_b (MV/m)	E_1 (MV/m)	E_2 (MV/m)	P_{max} (μC/cm^2)	P_r (μC/cm^2)	ΔP (μC/cm^2)
Pure PI	378	378	---	2.52	0.23	2.29
dPB	356	356	---	10.69	3.10	7.59
4dBP-8PI	424	158	557	8.11	0.91	7.20
8dBP-8PI	405	179	631	11.29	2.60	8.69
10dBP-8PI	364	171	605	11.61	3.19	8.42

Table S2. Comparison of energy density and efficiency of dielectric polymer composites

Composites	Energy density (J/cm^3)	Energy efficiency (%)	Electric field (MV/m)	References
PVDF/BT nws // E	10.8	61.4	240	1
PVDF/TiO_2(Array-1)	8.9	41.4	505	2
P(VDF-TrFE-CTFE)/TiO_2@PZT	6.9	---	143	3
PVDF/BST	13.1	69	340	4
P(VDF-HFP)/NBR (2 wt%)	11.3	73.3	500	5
PEI-10 vol% $BaTiO_3$/P(VDF-HFP)	6.0	96.8	450	6
PS/TiO_2/Al_2O_3	4.43	90	550	7
P(VDF-TrFE-CFE)/PMMA-15 wt%	9.3	73	520	8
P(VDF-TrFE-CFE)	5.4	---	270	8
Trilayered DE/P(VDF–HFP)	11.8	89	300	9
C01-3	9.73	---	453	10
TO-np/PVDF-BSBT-nf/PVDF-TO-np/PVDF	7.99	---	300	11
$BaTiO_3$-3wt%BN/PVDF	16.1	57	500.3	12
PET/BNNS-d12.14	8.77	96.5	736	13
DGM	19.68	71	700	14
4dBP-8PI	14.1	72	424	This work
8dBP-8PI	15.8	56	403	This work
10dBP-8PI	13.7	50	364	This work

References

1. B. Xie, H. Zhang, Q. Zhang, J. Zang, C. Yang, Q. Wang, M.-Y. Li and S. Jiang, *J. Mater. Chem. A*, 2017, **5**, 6070-6078.
2. D. Zhang, W. Liu, L. Tang, K. Zhou and H. Luo, *Appl. Phys. Lett.*, 2017, **110**, 133902.
3. D. Zhang, W. Liu, R. Guo, K. Zhou and H. Luo, *Adv. Sci.*, 2018, **5**, 1700512.
4. L. Yao, S. Wu, Z. Pan, Y. Tan, F. Pi, R. Wang, J. Zhai and H. H. D. Chen, *Mater. Des.*, 2020, **195**, 109044.
5. Q.-K. Feng, J.-Y. Pei, Y.-X. Zhang, D.-L. Zhang, D.-F. Liu, J.-B. Ping and Z.-M. Dang, *Compos. Sci. Technol.*, 2022, **226**, 109545.
6. L. Sun, Z. Shi, H. Wang, K. Zhang, D. Dastan, K. Sun and R. Fan, *J. Mater. Chem. A*, 2020, **8**, 5750-5757.
7. H. Li, B. Yao, Y. Zhou, W. Xu, L. Ren, D. Ai and Q. Wang, *ACS Appl. Energy Mater.*, 2020, **3**, 8055-8063.
8. Y. Zhu, P. Jiang and X. Huang, *Compos. Sci. Technol.*, 2019, **179**, 115-124.
9. J. Chen, Y. Wang, X. Xu, Q. Yuan, Y. Niu, Q. Wang and H. Wang, *J. Mater. Chem. A*, 2019, **7**, 3729-3736.
10. P. Hu, Y. Shen, Y. Guan, X. Zhang, Y. Lin, Q. Zhang and C.-W. Nan, *Adv. Funct. Mater.*, 2014, **24**, 3172-3178.
11. P. Hu, J. Wang, Y. Shen, Y. Guan, Y. Lin and C.-W. Nan, *J. Mater. Chem. A*, 2013, **1**, 12321-12326.
12. R. Guo, H. Luo, D. Zhai, Z. Xiao, H. Xie, Y. Liu, X. Zhou and D. Zhang, *Chem. Eng. J.*, 2022, **437**, 135497.
13. J.-B. Ping, Q.-K. Feng, Y.-X. Zhang, X.-J. Wang, L. Huang, S.-L. Zhong and Z.-M. Dang, *Nano Micro Lett.*, 2023, **15**, 154.
14. Y. Liu, G. Tian, Y. Sun, S. Wang, L. Huang, X. Li, T. Xu, L. Jin, Y. Zou, W. Deng and W. Yang, *Small*, 2025, **21**, 2411304.